

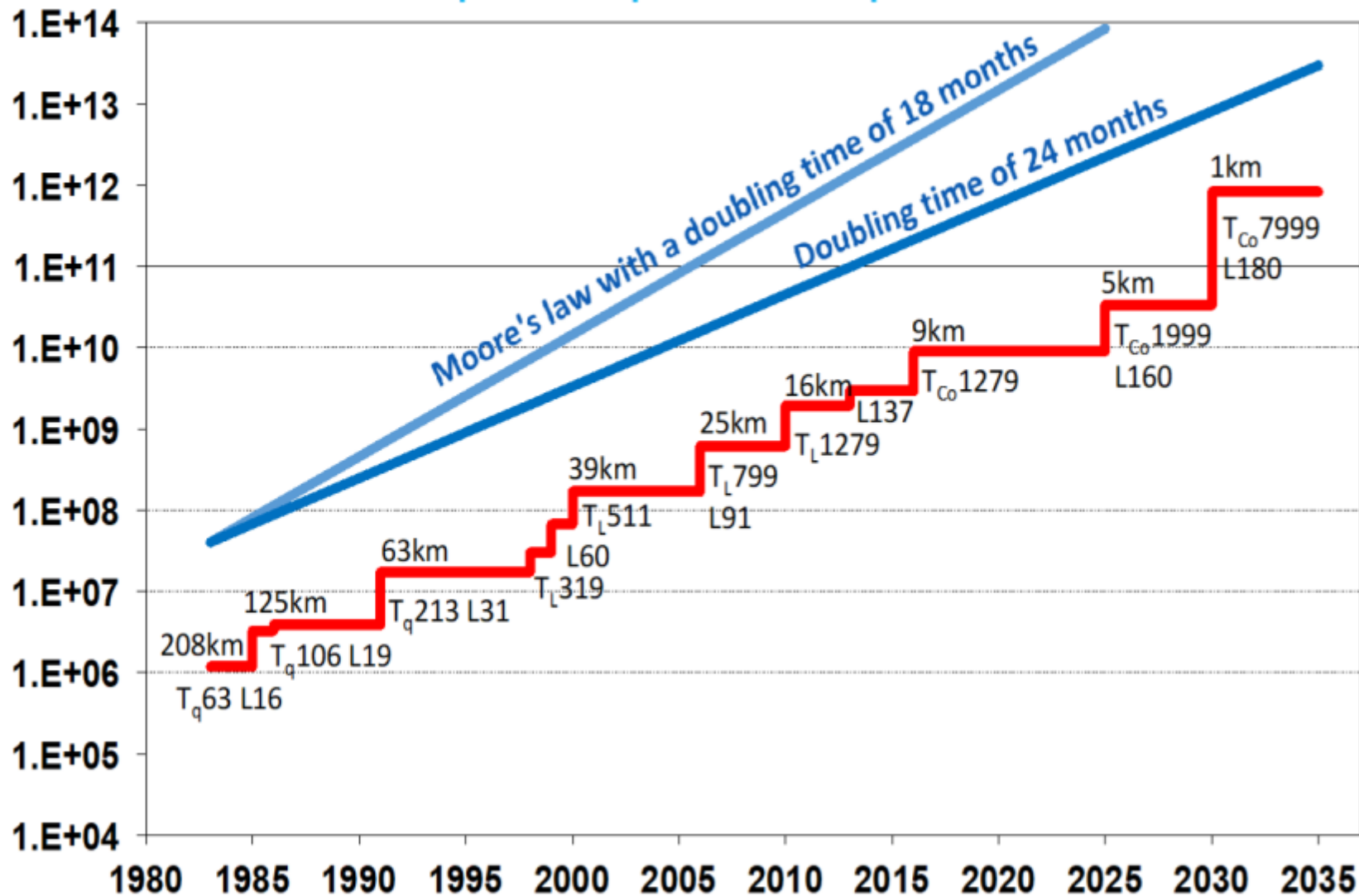
The Integrated Forecasting System (IFS)

Nils P. Wedi

European Centre for Medium-Range Weather Forecasts (ECMWF)



Computational power drives spatial resolution



(Schulthess et al, 2019)

ECMWF's progress in degrees of freedom
(levels x grid columns x prognostic variables)

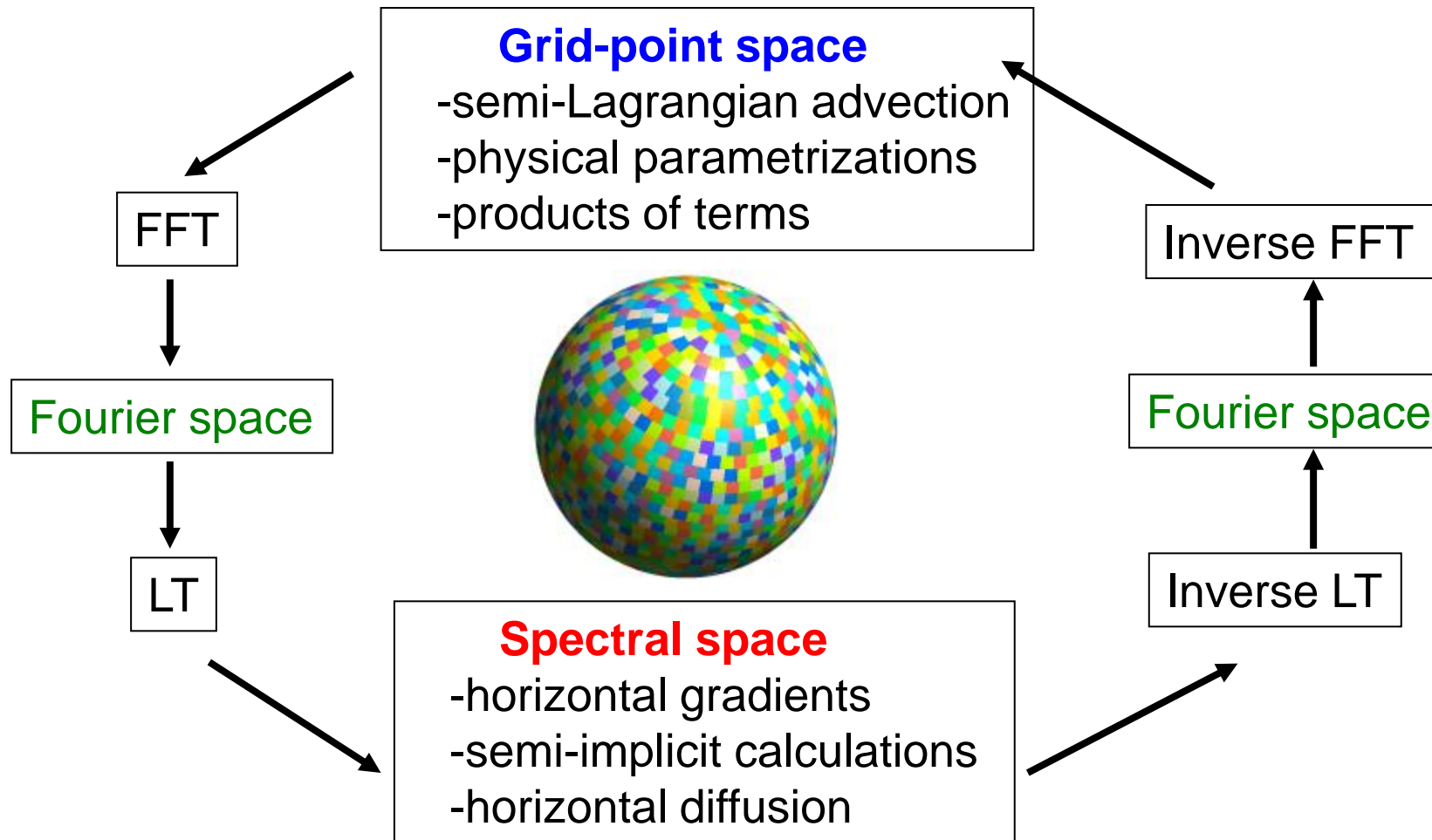
IFS dynamical core options

Model aspect	IFS-FVM	IFS-ST	IFS-ST (NH option)
Equation system	fully compressible	hydrostatic primitive	fully compressible
Prognostic variables	$\rho_d, u, v, w, \theta', \varphi', r_v, r_l, r_r, r_i, r_s$	$\ln p_s, u, v, T_v, q_v, q_l, q_r, q_i, q_s$	$\ln \pi_s, u, v, d_4, T_v, \hat{q}, q_v, q_l, q_r, q_i, q_s$
Horizontal coordinates	λ, ϕ (lon–lat)	λ, ϕ (lon–lat)	λ, ϕ (lon–lat)
Vertical coordinate	generalized height	hybrid sigma–pressure	hybrid sigma–pressure
Horizontal discretization	unstructured finite volume (FV)	spectral transform (ST)	spectral transform (ST)
Vertical discretization	structured FD–FV	structured FE	structured FD or FE
Horizontal staggering	co-located	co-located	co-located
Vertical staggering	co-located	co-located	co-located, Lorenz
Horizontal grid	octahedral Gaussian or arbitrary	octahedral Gaussian	octahedral Gaussian
Time stepping scheme	2-TL SI	2-TL constant-coefficient SI	2-TL constant-coefficient SI with ICI
Advection	conservative FV Eulerian	non-conservative SL	non-conservative SL

Dyamond configuration

(Kühnlein et al, 2019)

Schematic description of the *spectral transform method* in the ECMWF IFS model

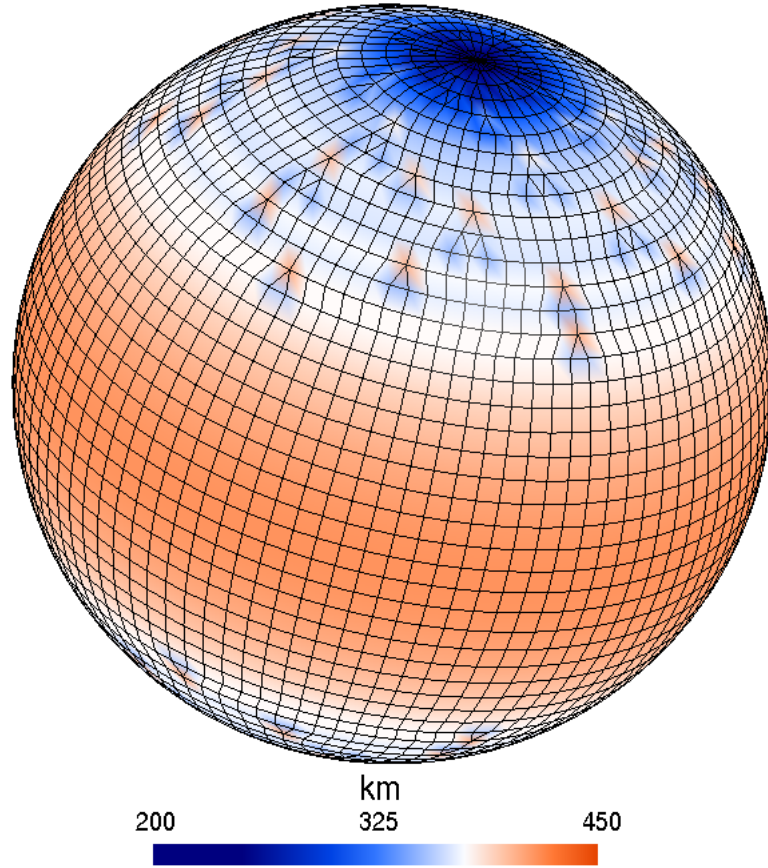


FFT: Fast Fourier Transform, LT: Legendre Transform

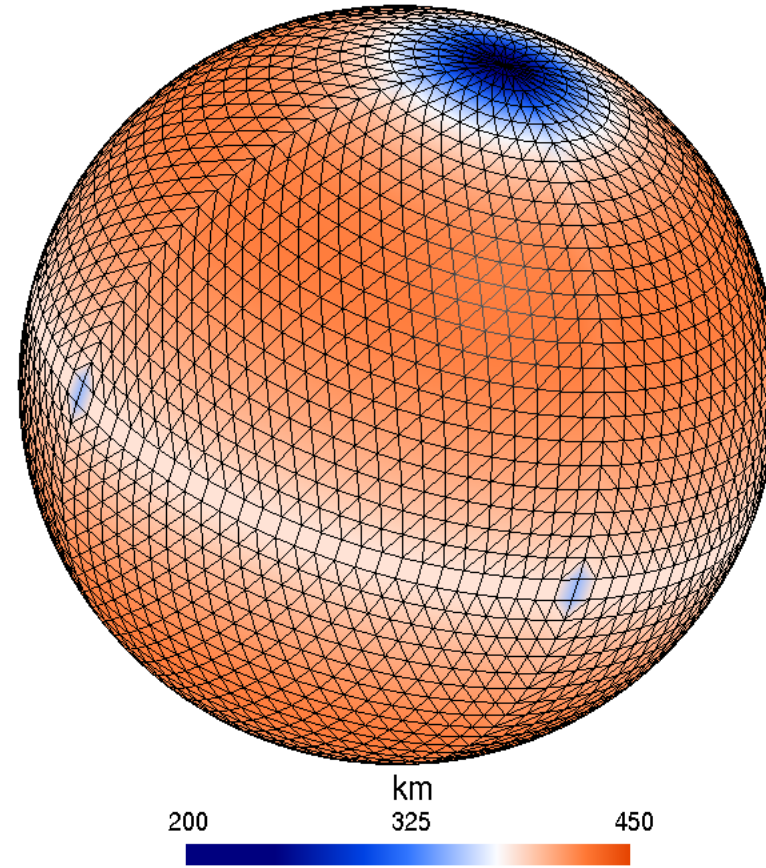
The IFS model grid

Integrated Forecasting System (IFS)

A further ~20% reduction in gridpoints
=> ~50% less points compared to full grid



N24 reduced Gaussian grid

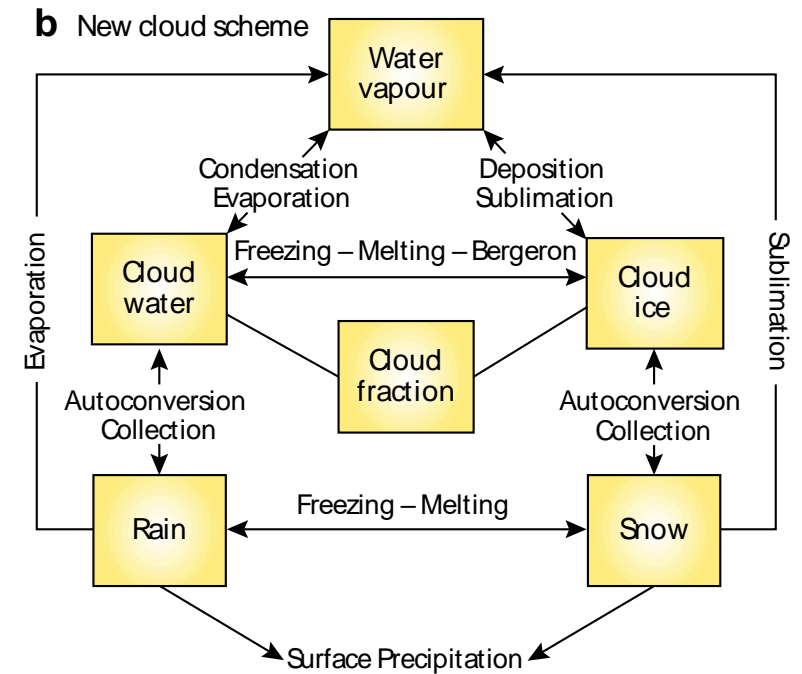


N24 octahedral Gaussian grid

(Wedi et al, 2014, 2015; Malardel et al, 2015; Deconinck et al, 2017)

Parametrizations

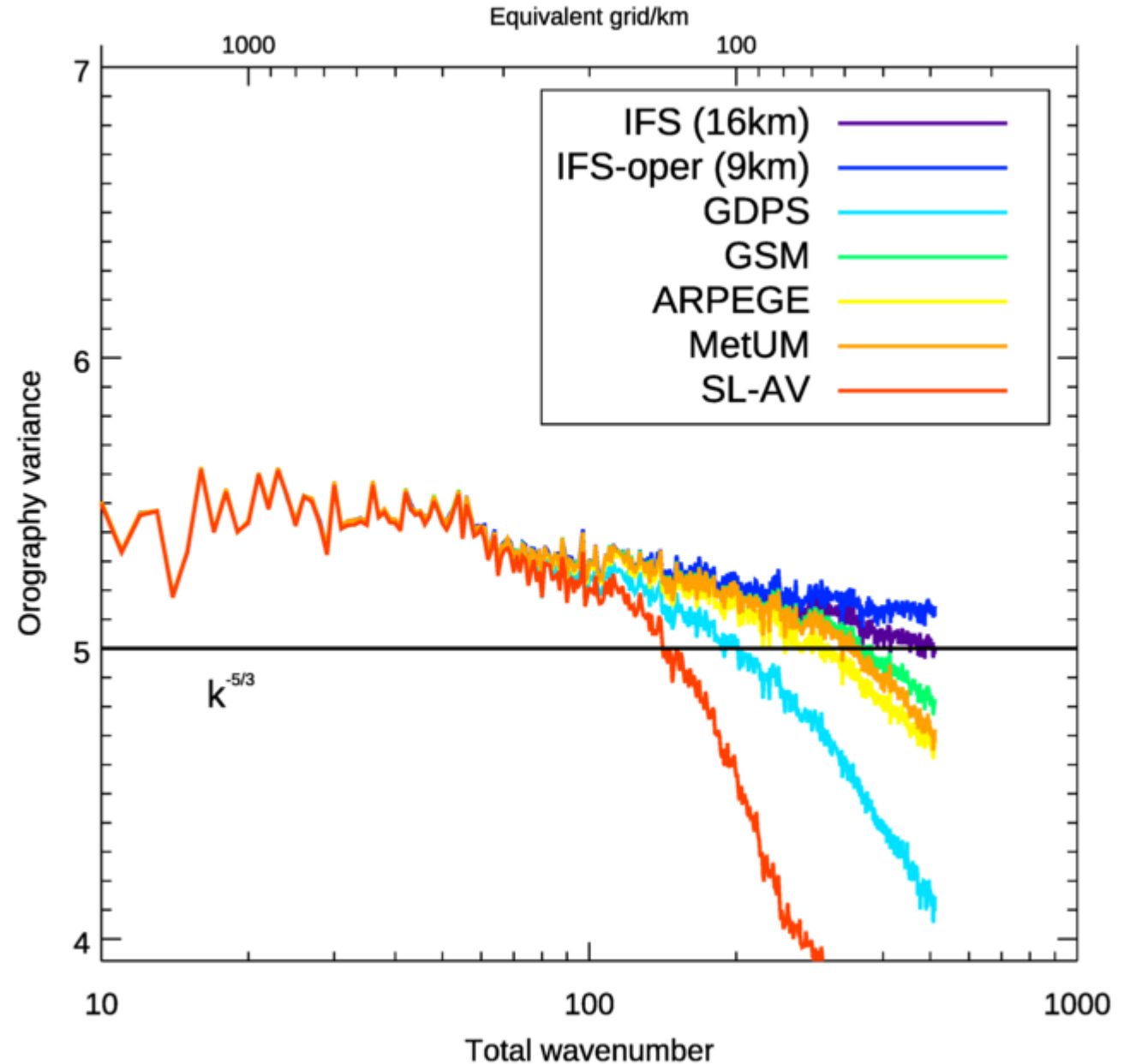
- Shallow, (deep) and midlevel convection, bulk mass flux scheme (Tiedke, 1988; Bechtold, 2008, 2014)
- Single moment cloud microphysics scheme (Tiedke, 1993; Forbes et al, 2011)
- PBL scheme and coupling to TOFD and dynamics (Beljaars, 1991; 2018)
- Orographic gravity wave drag and TOFD (Beljaars et al, 2004)
- Non-orographic drag (Orr et al, 2010)
- Radiation (10km grid in Dyamond; Hogan et al, 2018)
- Ocean waves (0.25 degrees ECWAM; Janssen et al, 2018)



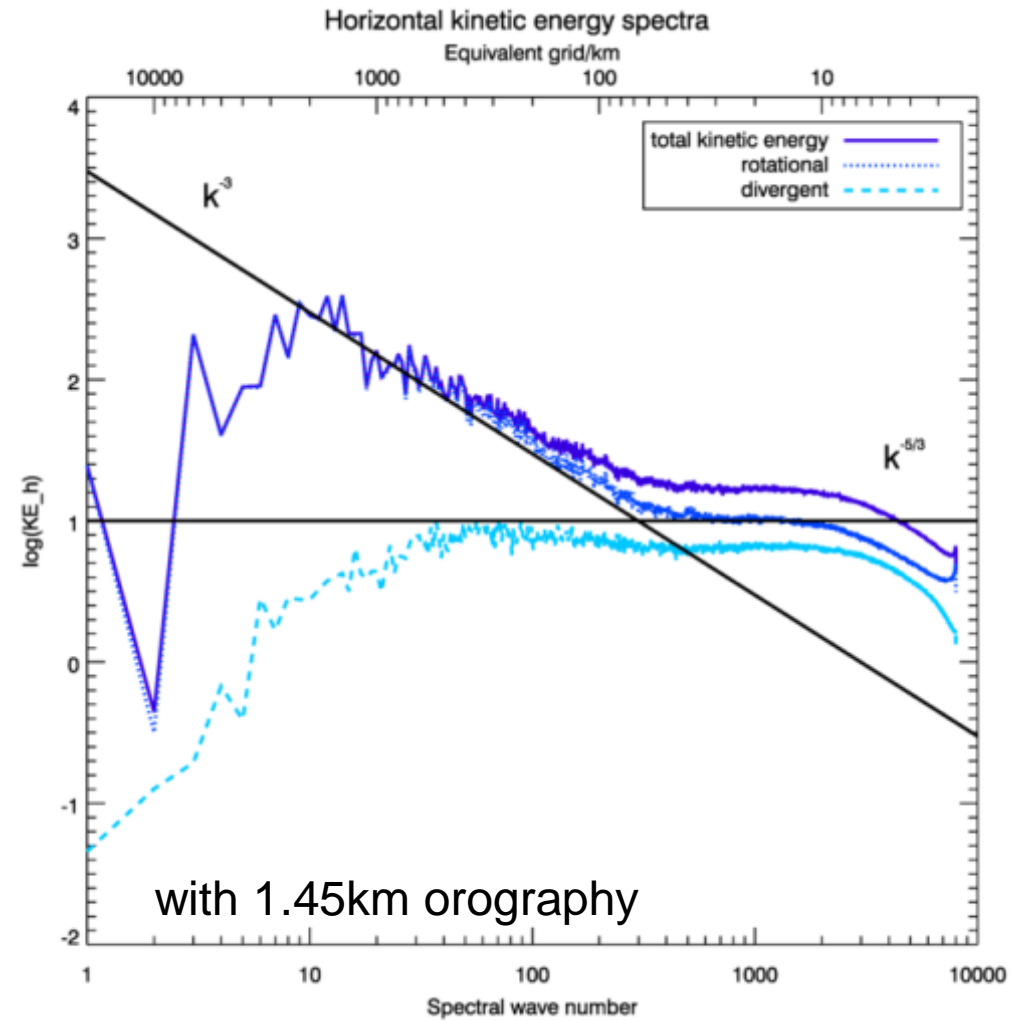
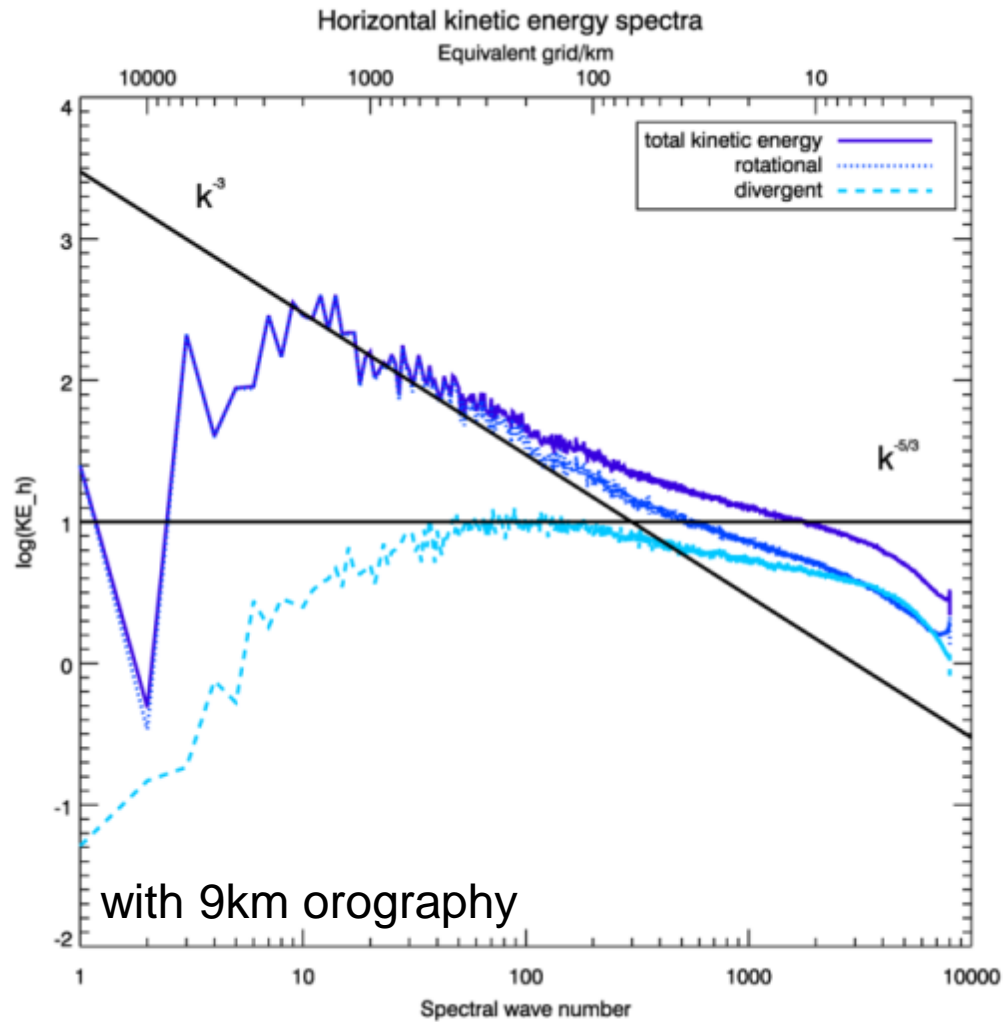
Orography representation

- Differences in orography (and associated filters applied) have a significant impact on surface stresses and circulation patterns on weather & climate models.

Elvidge et al 2019



Global 1.45km spectra: Mid-Troposphere 500hPa



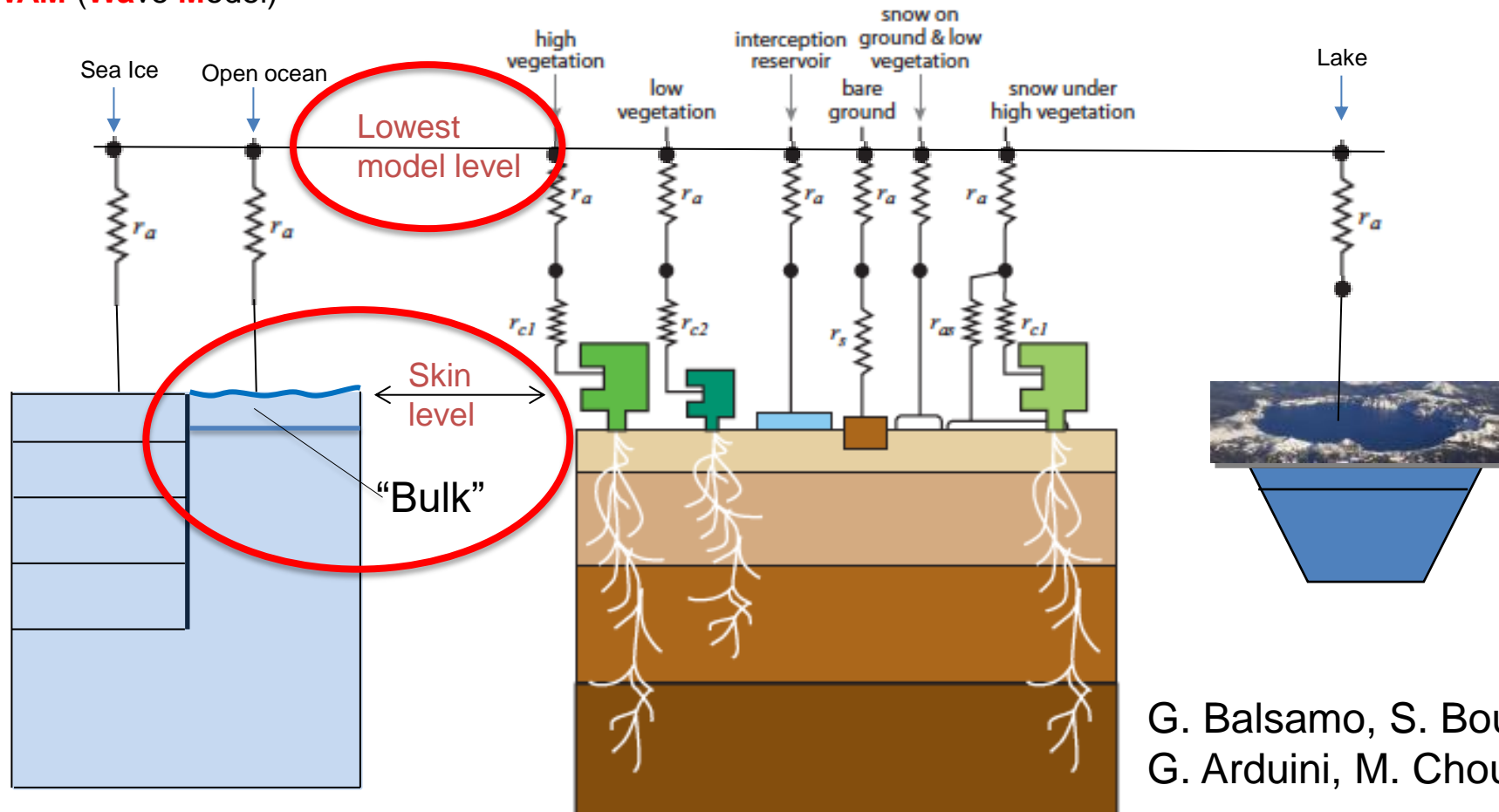
Impact of parametrizations + orography, (*Malardel + Wedi, JGR 2016*)

The tile scheme allows for a simple representation of **surface heterogeneity** over land and for fractional sea ice over the ocean

NEMO (Nucleus for European Modelling of the Ocean) + **WAM** (Wave Model)

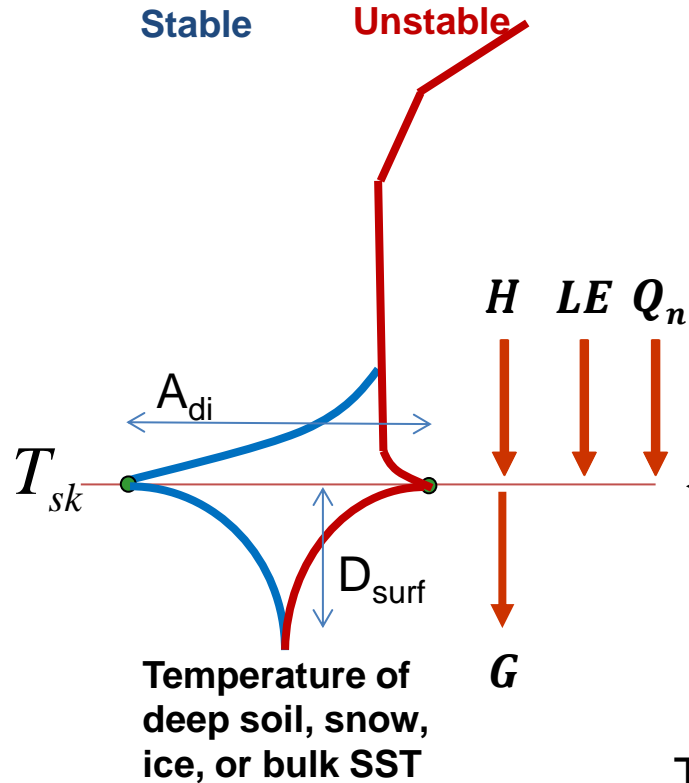
HTESSEL (Hydrology -Tiled ECMWF Scheme for Surface Exchanges over Land)

FLAKE (Fresh water Lake scheme)



G. Balsamo, S. Boussetta,
G. Arduini, M. Choulga, A. Beljaars,
...

Typical near surface diurnal cycle structure of temperature profiles



Surface energy balance:

$$Q_n + H + LE = G$$

Q_n : Net radiation (solar + thermal)

H : Sensible heat flux

LE : Latent heat flux

G : Heat flux into the surface

T_{sk} : Radiation intercepting/emitting level, e.g. SST, ice surface, vegetation canopy, litter layer on top of bare soil, top of snow layer, or combination of these in a heterogeneous configuration

Typical numbers

	A_{di} (K) Diurnal cycle amplitude of T_{sk}	D_{surf} (cm) Surface penetration depth of diurnal cycle
Land	10 - 30	10
Snow	0 - 10	5
Ice	0 - 10	10
Open ocean	0 - 2	100

Anton Beljaars

Vertical surface fluxes

friction velocity² (correlated with momentum flux)

$$u_*^2 = \left[\frac{\kappa^2}{\ln^2(z_1/z_{0m})} \right] * F_m(z_{0m}, z_{0h}, Rib) * |v_1|^2$$

Roughness lengths

$$z_{0m} = \delta * \nu / u_* + \alpha u_*^2 / g$$

$$z_{0h} = \delta * \nu / u_*$$

Lowest model level
or 10m wind speed

latent heat flux

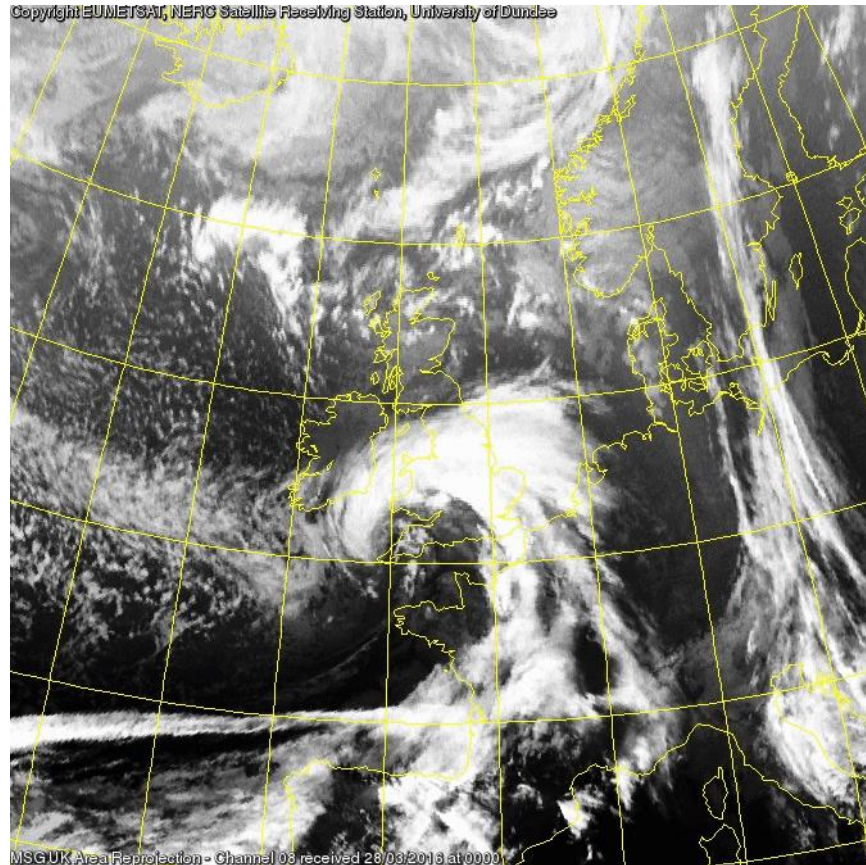
$$\overline{w'q'_0} = \left[\frac{\kappa^2}{\ln(z_1/z_{0m}) \ln(z_1/z_{0q})} \right] * F_q(z_{0m}, z_{0q}, Rib) * |v_1| * (q_S - q_1)$$

sensible heat flux

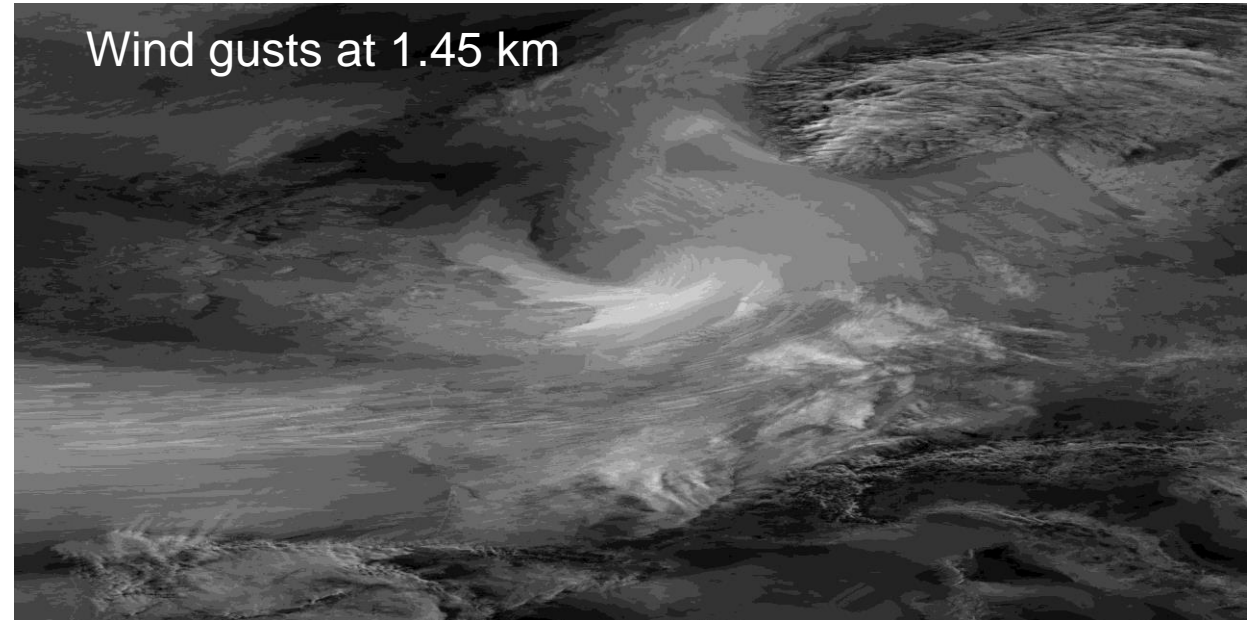
$$\overline{w'\theta'_0} = \left[\frac{\kappa^2}{\ln(z_1/z_{0m}) \ln(z_1/z_{0h})} \right] * F_h(z_{0m}, z_{0h}, Rib) * |v_1| * (\theta_S - \theta_1)$$

Improved surface boundary layer description

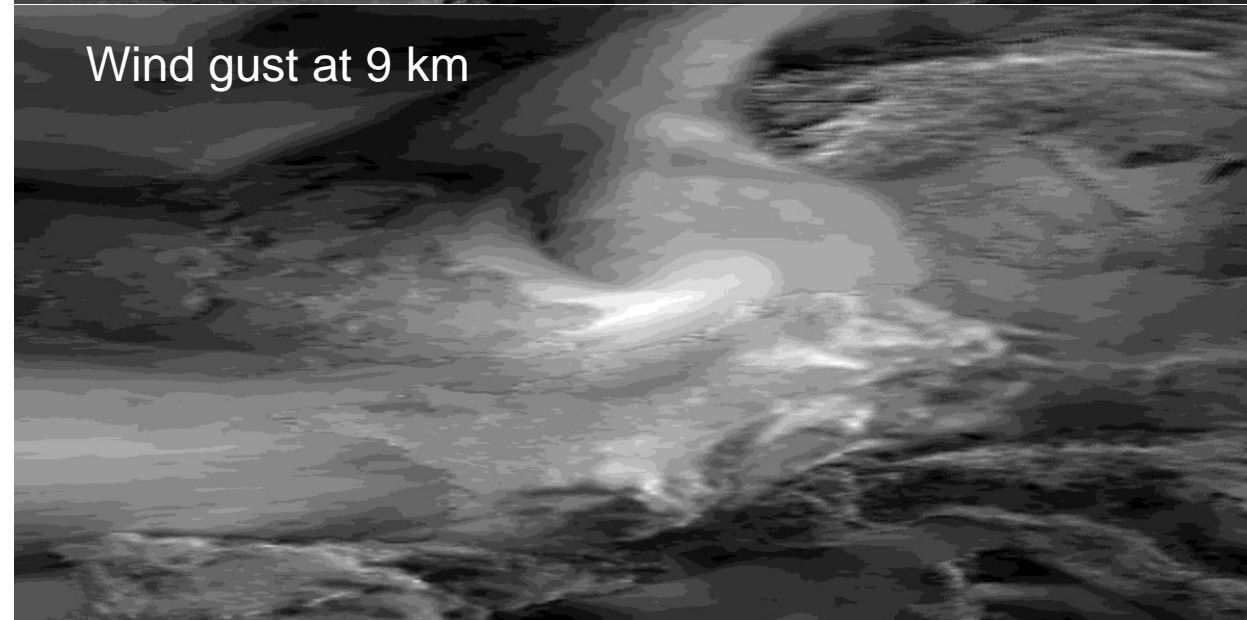
... wind gust details at 1.45km



Wind gusts at 1.45 km



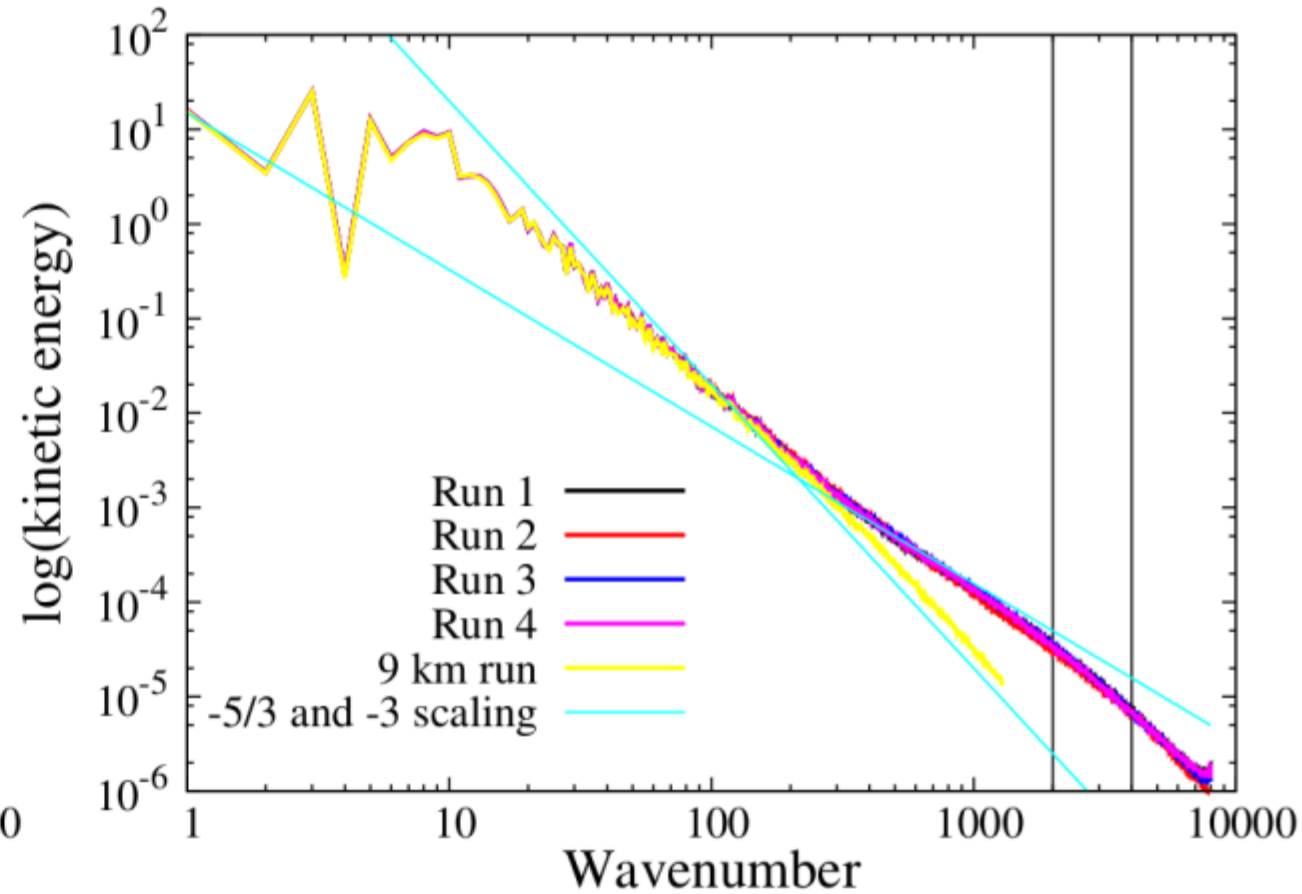
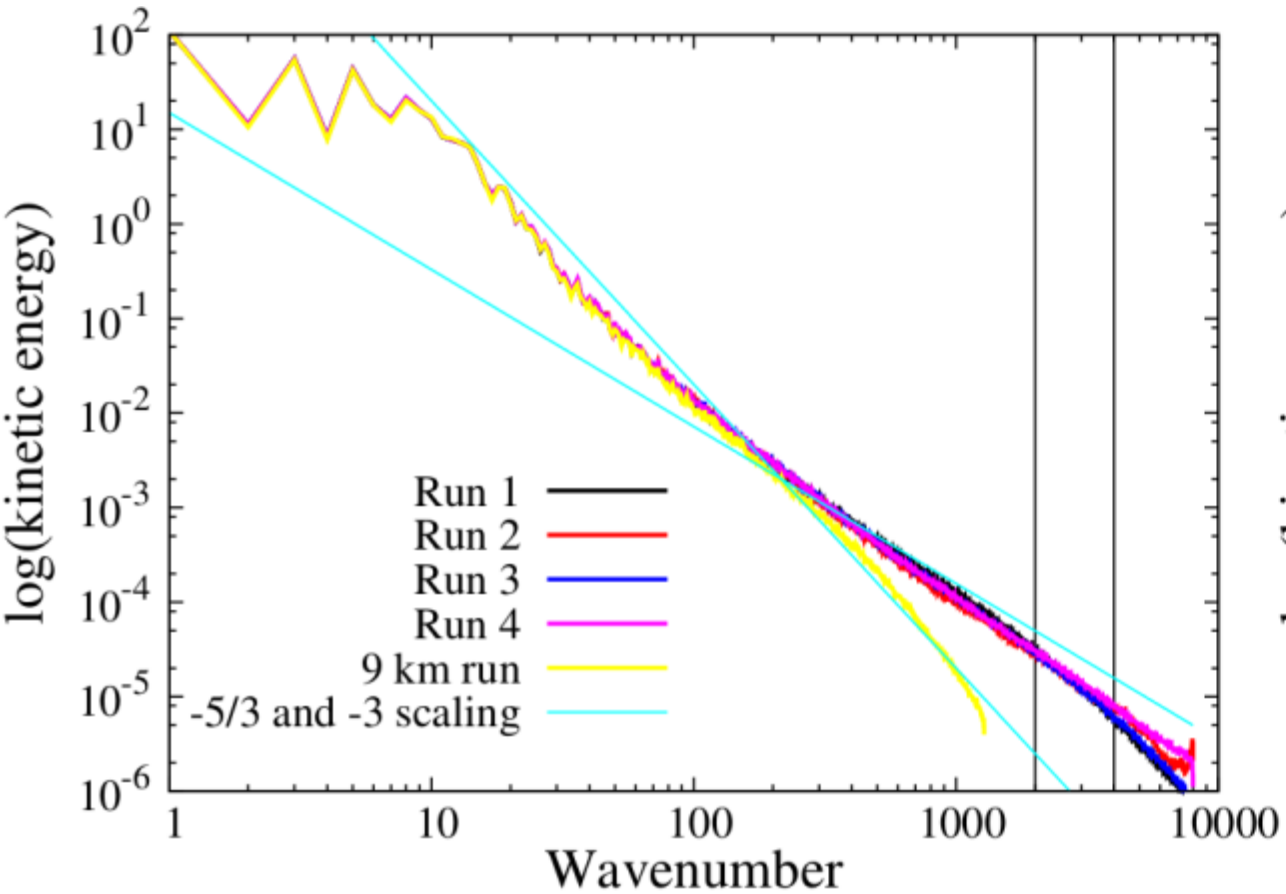
Wind gust at 9 km



Global simulations at 1.45 km resolution

- We perform uncoupled (no ocean, no wave model) simulations with IFS.
- Weather simulations at full complexity including recent date initial conditions, real-world topography, state-of-the-art physical parametrizations and diabatic forcing including shallow convection, turbulent diffusion, radiation and five categories for the water substance (vapour, liquid, rain, ice, snow)
- Simulations with 62 and 137 vertical levels
- Simulations with hydrostatic and non-hydrostatic equations

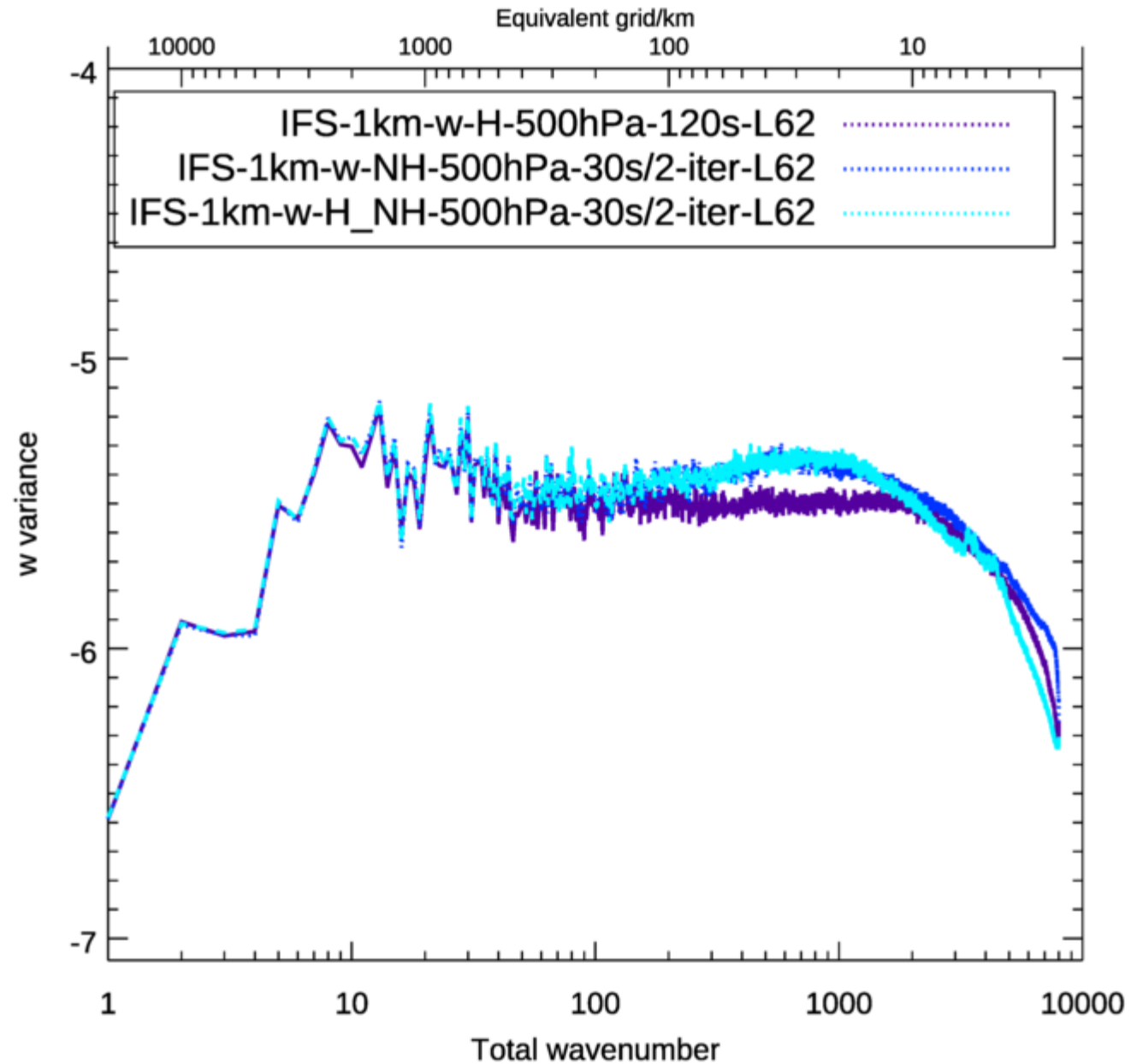
Energy spectra



- The spectra @1.45 km are reasonable and show clear improvements compared to a simulations at 9 km.
- Effective resolutions is between 5 and 10 km.

IFS vertical velocity spectra 500hPa at 1.45 km H vs NH

T+48h



Vertical velocity [m/s]

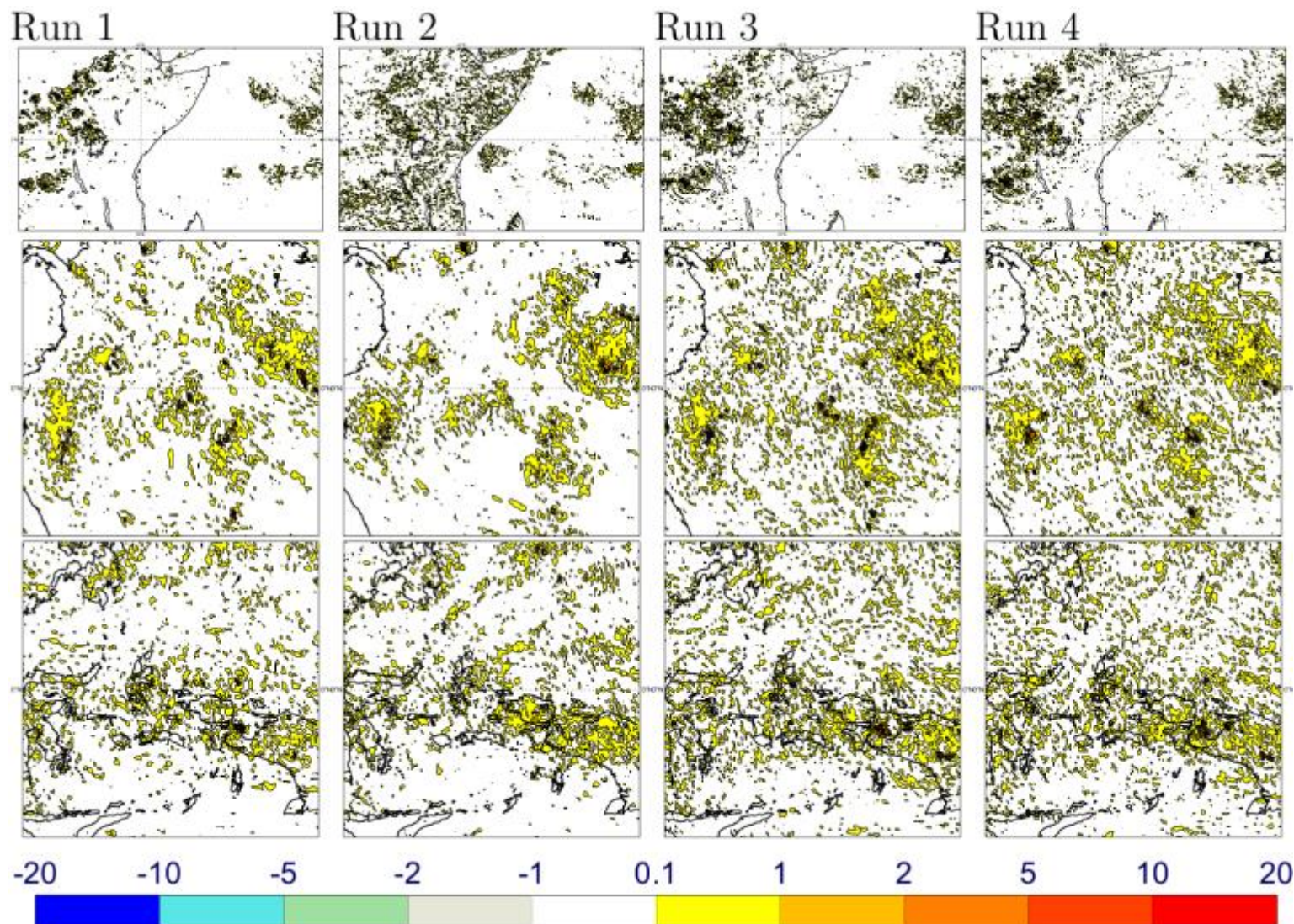
Run 1: H, 120s, 0PC; Run 2: NH, 120s, 1PC; Run 3: H, 30s, 2PC; Run 4: NH, 30s, 2PC

- Run 1 shows the smallest area with strong convection
 - Run 1 and 2 are similar
 - Run 3 and 4 are similar
- > small differences between H and NH
-> large differences as function of time step choice

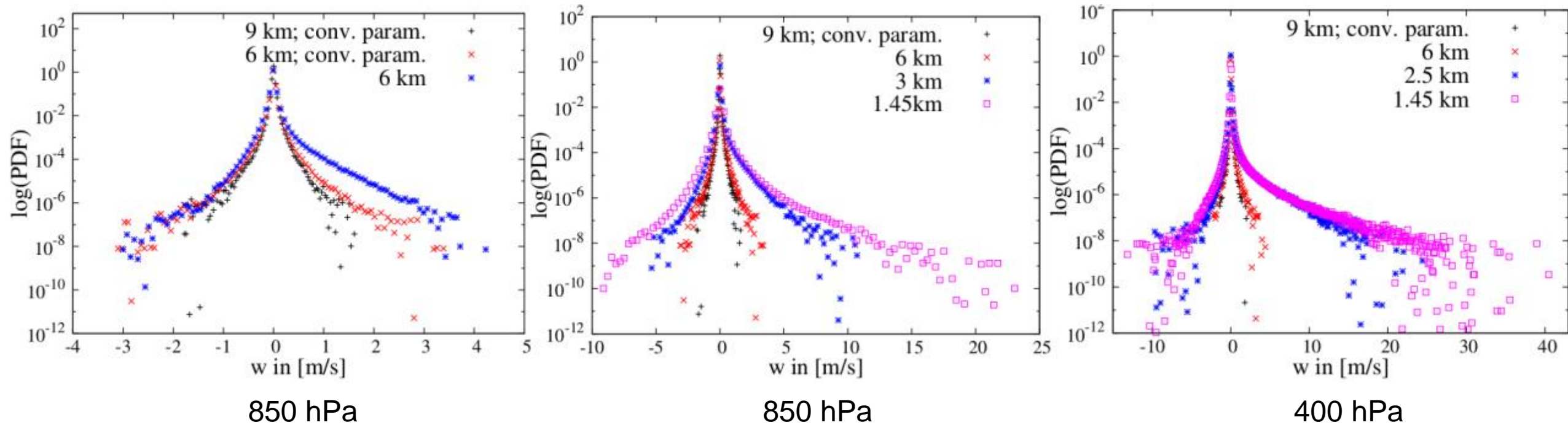
East Africa

South America

Indonesia



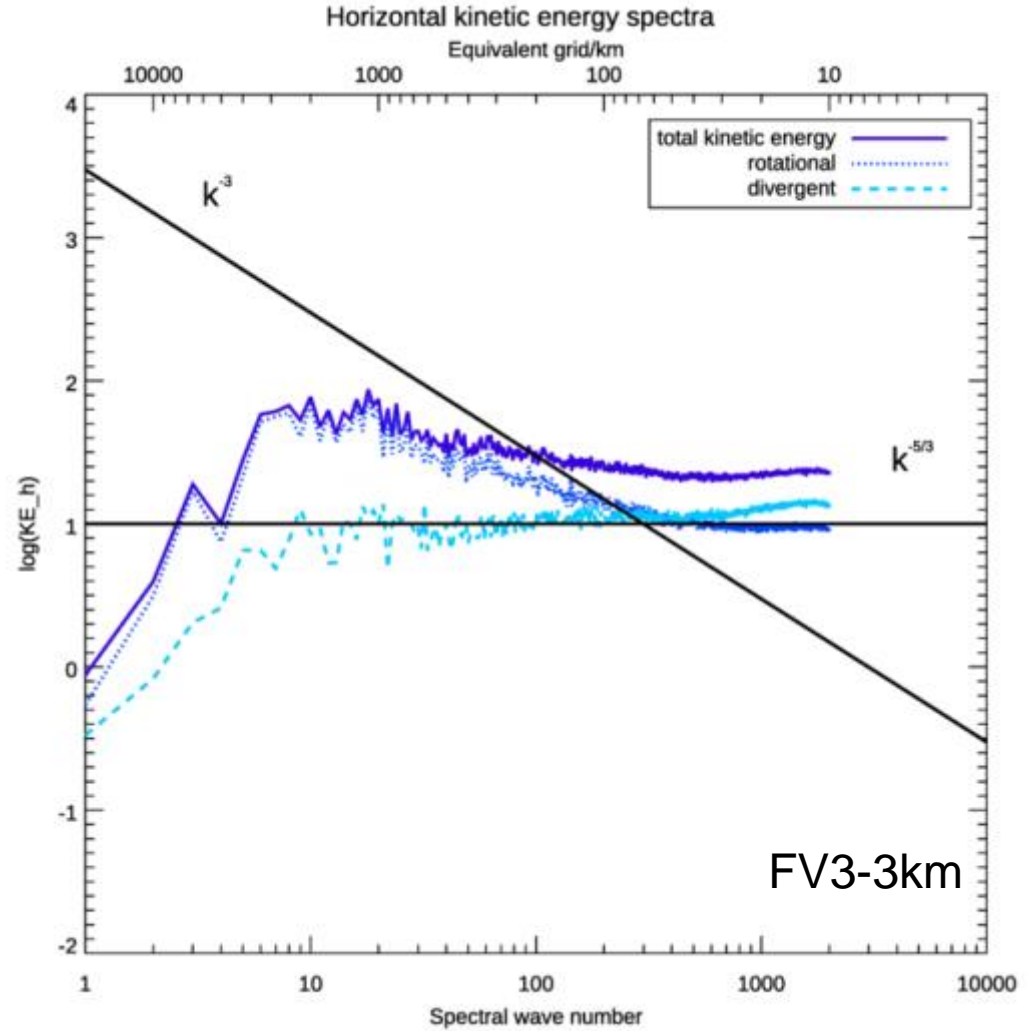
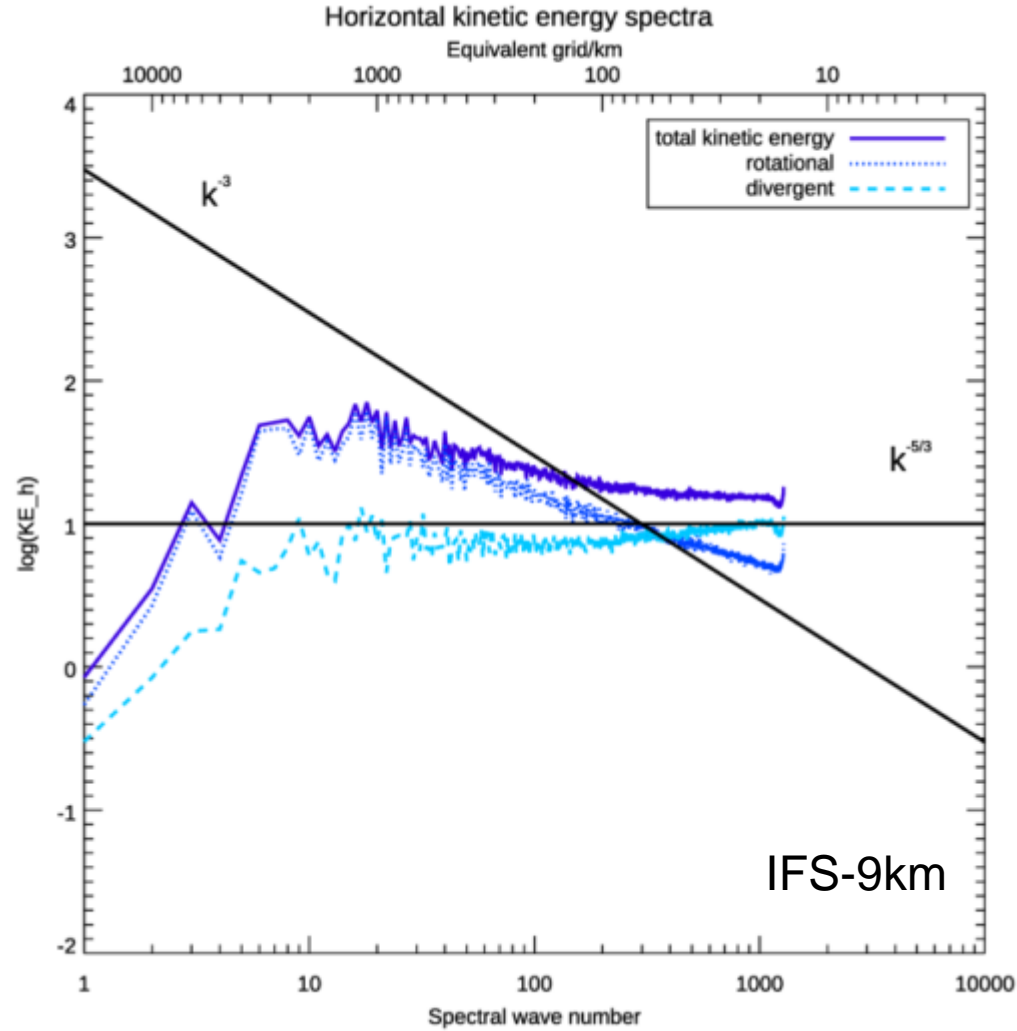
PDFs of vertical velocity – Impact of resolution



- Please note the logarithm on the y-axis.
- Distributions are symmetric if deep convection is parametrised.
- There are stronger upward velocities if convection is represented explicitly.
- Extreme velocities increase as resolution is increasing.

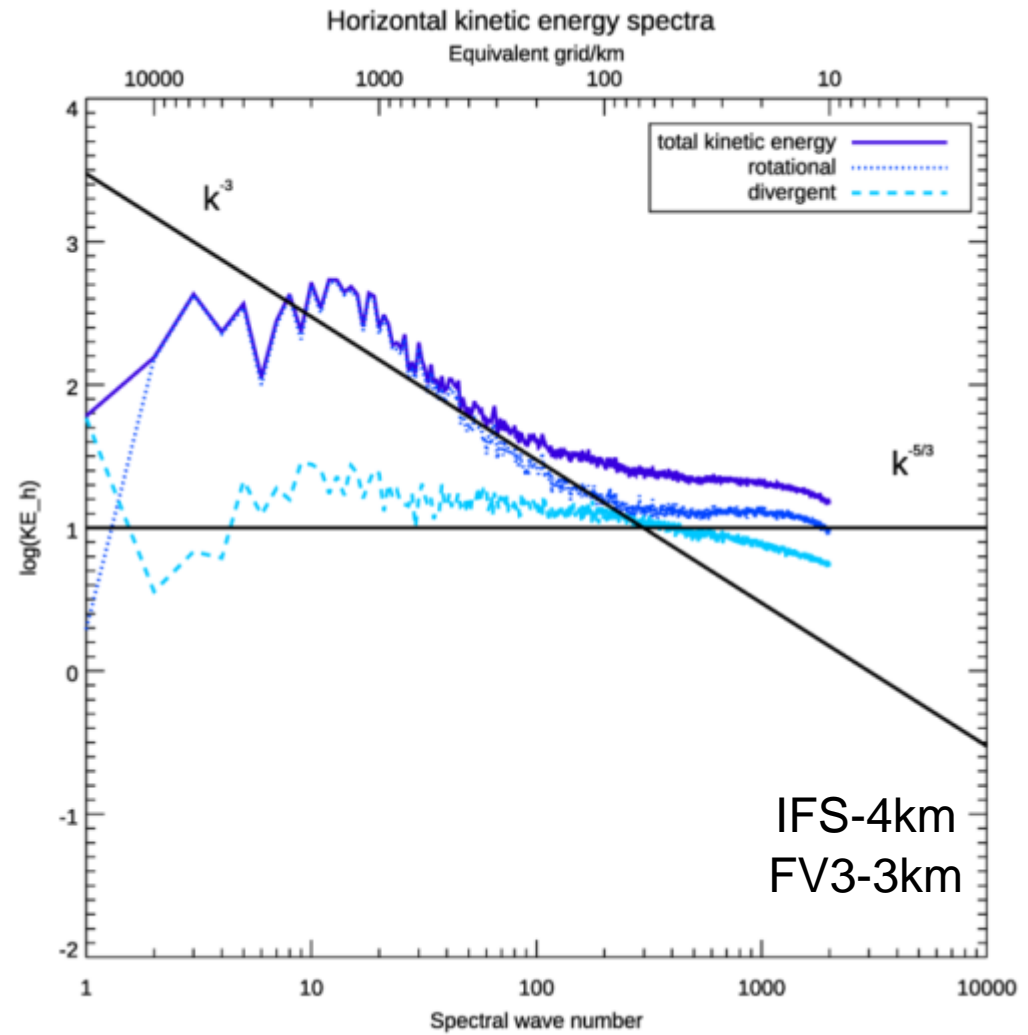
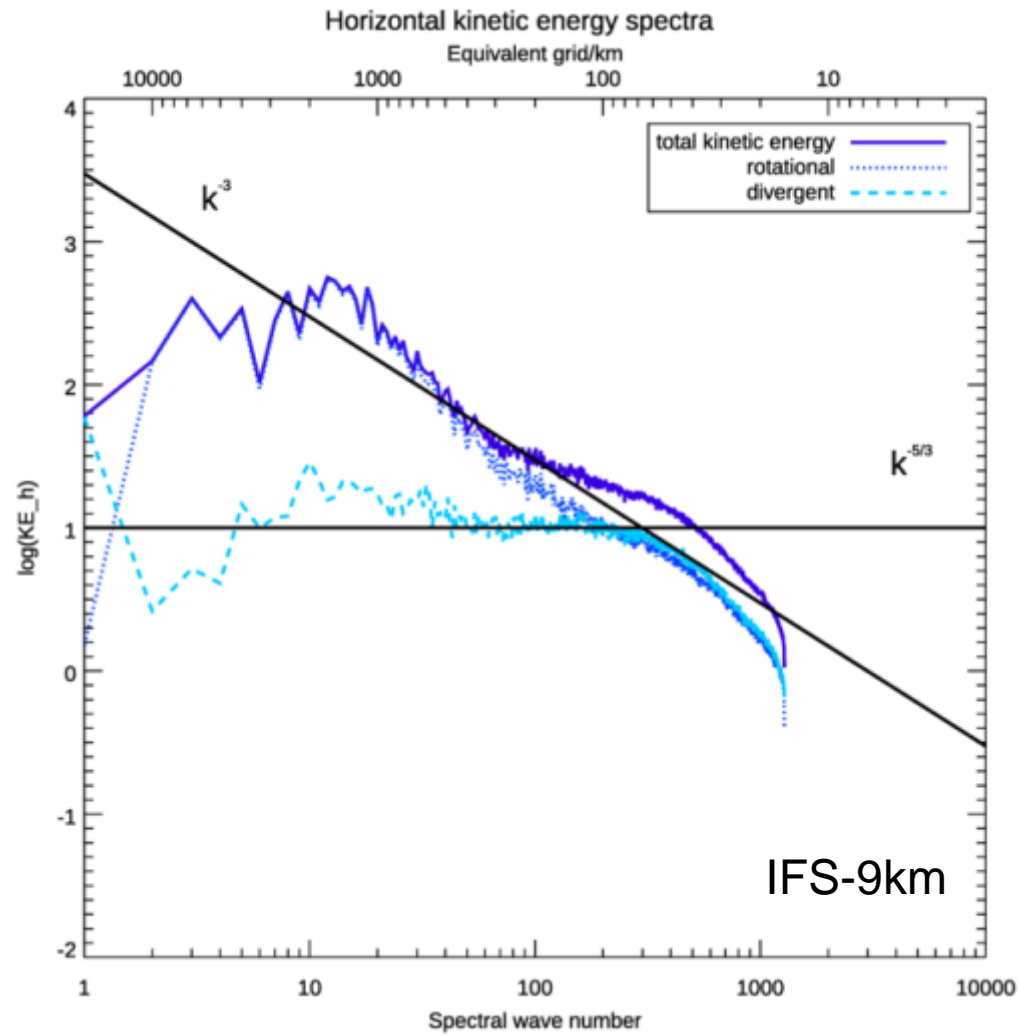
IFS vs FV3 kinetic energy spectra sfc

T+48h



IFS vs FV3 kinetic energy spectra 200hPa

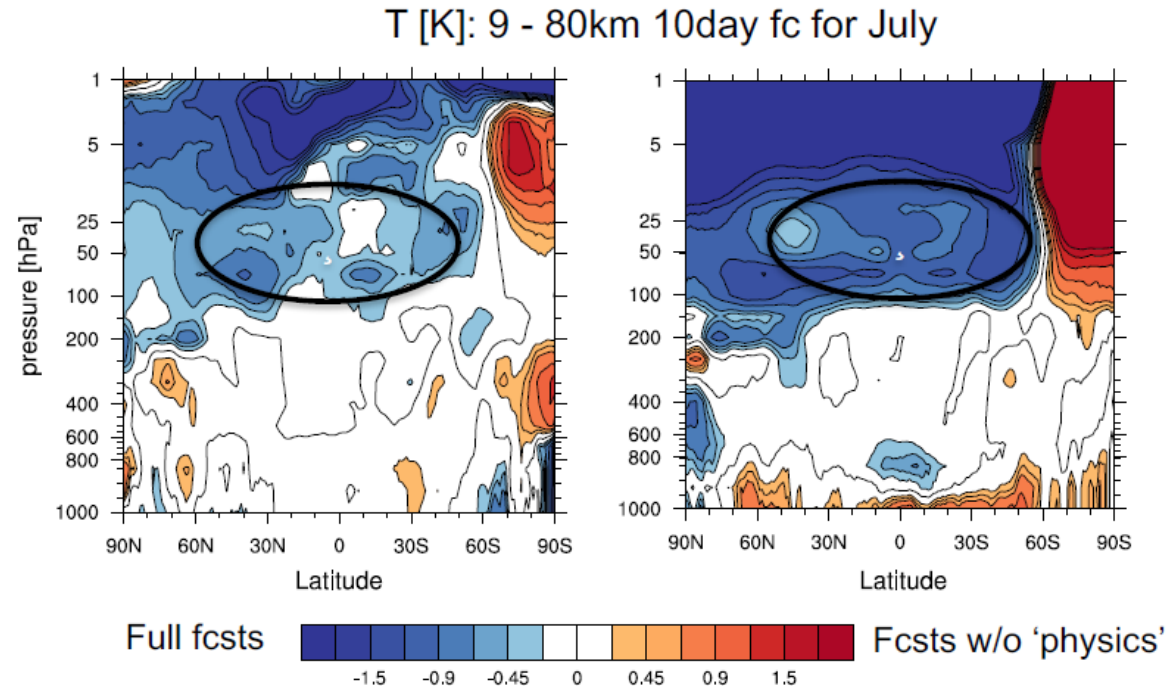
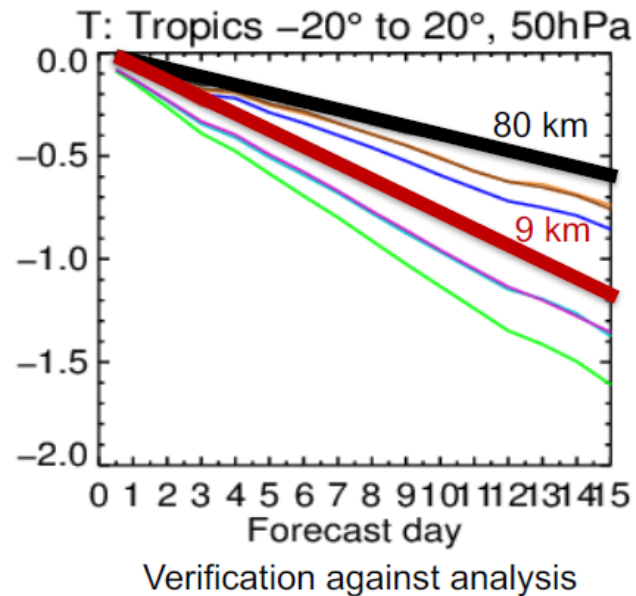
T+48h
Same initial conditions
Dyamond



Horizontal resolution sensitivity of temperature biases

Stratosphere cools in the global mean with increase in horizontal resolution → biases worse in the lower- to mid- stratosphere with increase in horizontal resolution. Affects all forecast ranges, from medium to seasonal.

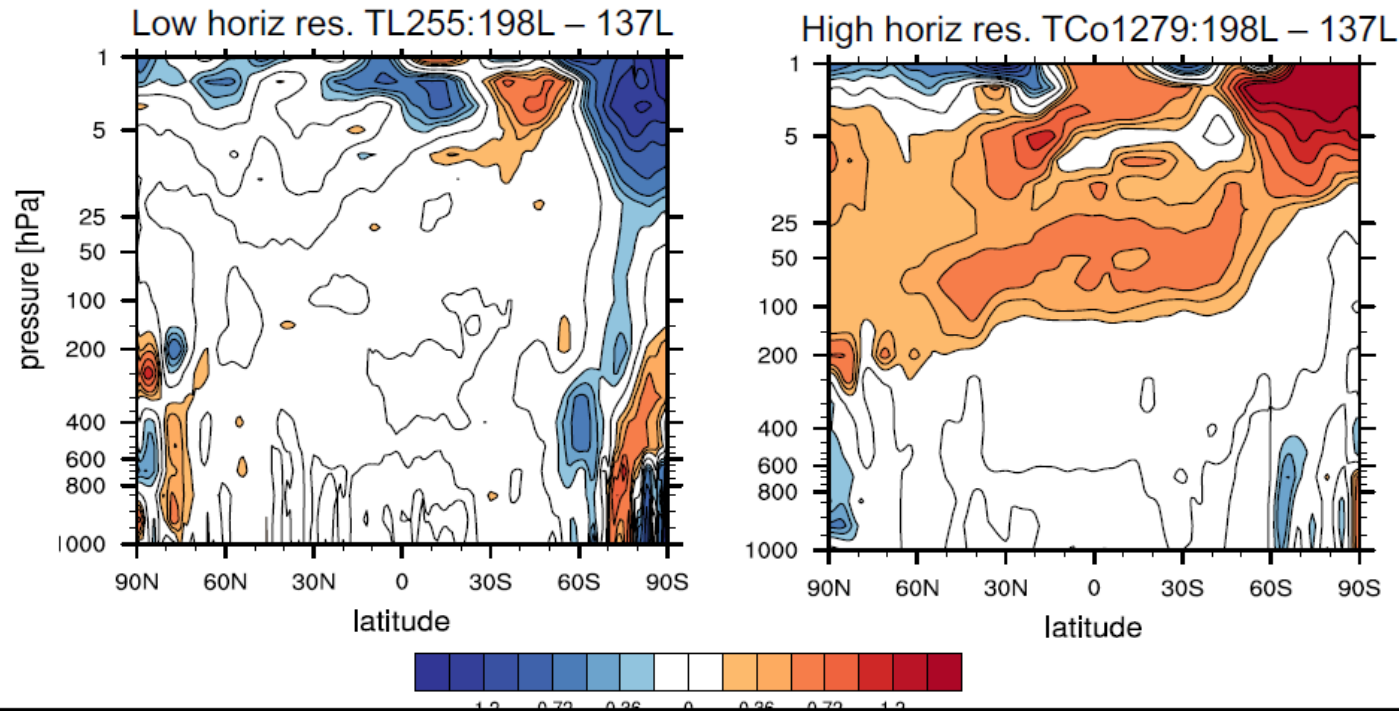
Resolved dynamics the culprit. Forecasts with no physical parametrizations, show the same horizontal resolution.



Vertical resolution sensitivity of temperature

Question: Does increasing **vertical resolution** eliminate the horizontal resolution sensitivity?

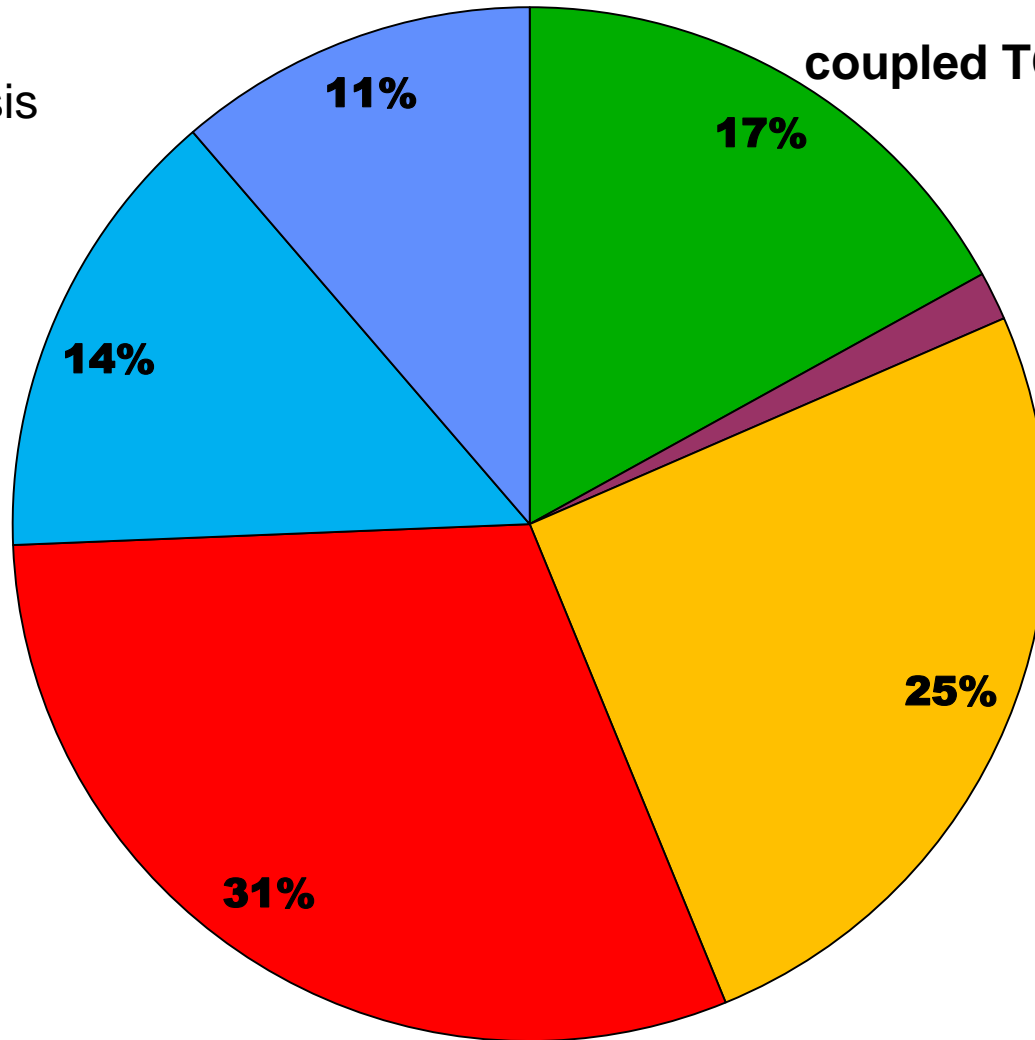
200m vertical resolution in the 150-50hPa region enough to eliminate horizontal resolution sensitivity (up to TCo1279 horizontal resolution).



Where do we spend the time (& energy) ? Cycle 45r1 operations

■ GP_DYNAMICS ■ SI_SOLVER ■ SP_TRANSFORMS ■ PHYSICS+RAD ■ WAVEMODEL ■ OCEANMODEL

Careful scalability analysis
of all ESM components!



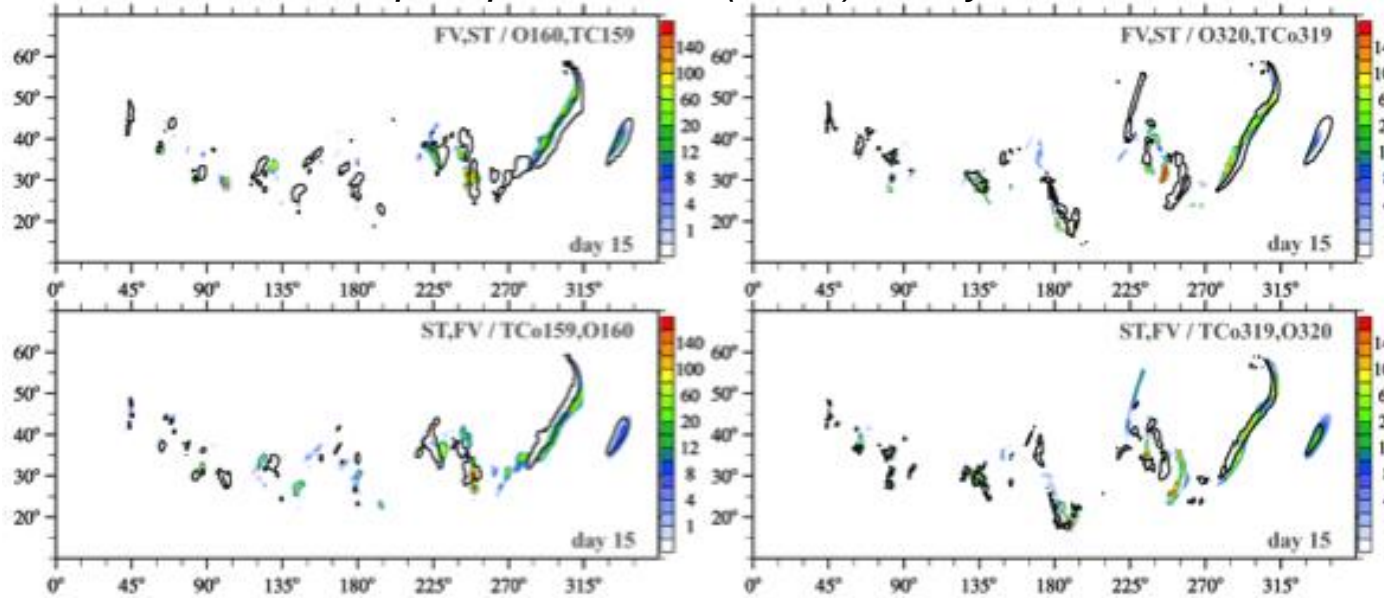
coupled TCo1279 L137 (~9km operational) run

Single electrical group:
~52 minutes wallclock time
(single electrical group==384 nodes)

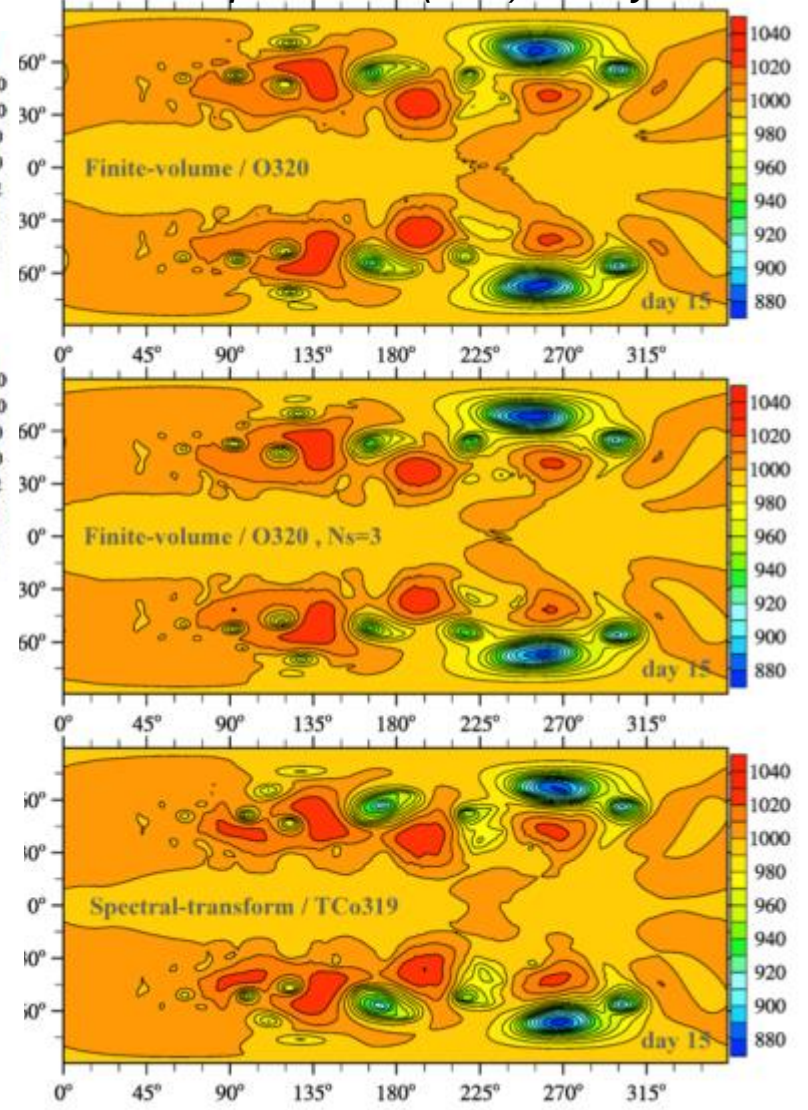
1408 MPI tasks x 18 threads
290 FC/day

IFS-FVM (finite-volume) comparison to hydrostatic IFS-ST: moist-precipitating dynamics and coupling to IFS physics parametrisations

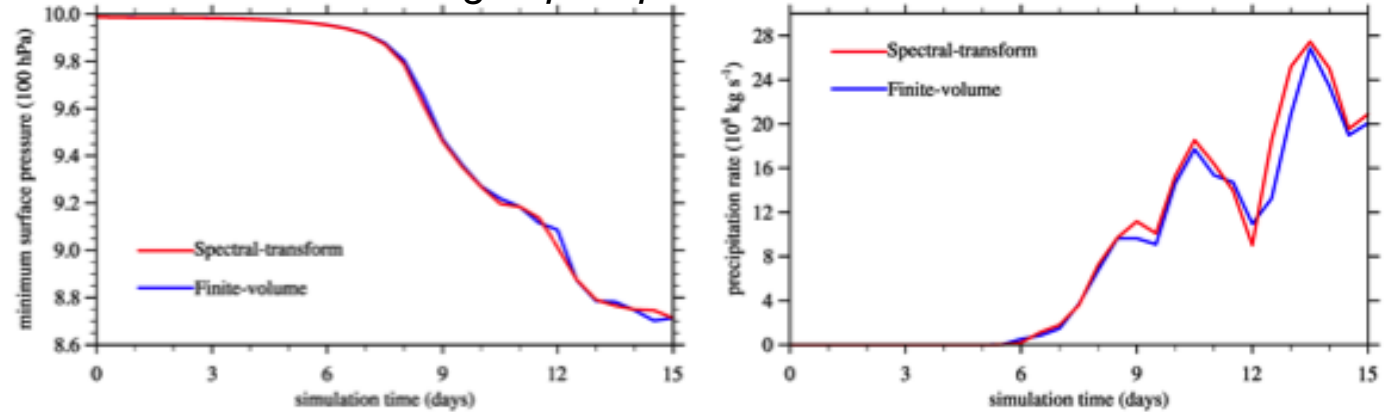
precipitation rate (mm/h) at day 15



surface pressure (hPa) at day 15



Area-averaged precipitation rate with simulation time



Data processing of Dyamond data

- Cdo tools (handling also gptosp and sptogp ?)
- Data size
 - Grib 16 bit per value storage; spectral data complex packing
 - 9km: 6.599.680 points
 - 4km: 26.306.560 points
 - 1.45km: 256.800.000 points



The ESIWACE project has received funding from the European Union's Horizon 2020 research and innovation programme under grant agreement No 675191.

Additional slides